Despite Impaired Binocular Function, Binocular Disparity Integration Across the Visual Field Is Spared in Normal Aging and Glaucoma

Guido Maiello[1] and MiYoung Kwon[2]

[1]School of Psychology, Faculty of Environmental and Life Sciences, University of Southampton, Southampton, United Kingdom
[2]Department of Psychology, Northeastern University, Boston, Massachusetts, United States

Correspondence: Guido Maiello, School of Psychology, Faculty of Environmental and Life Sciences, B44 University Rd, University of Southampton, Southampton SO17 1PS, Southampton, UK; g.maiello@soton.ac.uk; guido_maiello@yahoo.it. MiYoung Kwon, Department of Psychology, Northeastern University, 125 Nightingale Hall, 360 Huntington Ave., Boston, MA 02115, USA; m.kwon@northeastern.edu.

Received: February 8, 2023
Accepted: April 7, 2023
Published: May 2, 2023

Citation: Maiello G, Kwon M. Despite impaired binocular function, binocular disparity integration across the visual field is spared in normal aging and glaucoma. *Invest Ophthalmol Vis Sci.* 2023;64(5):2. https://doi.org/10.1167/iovs.64.5.2

Purpose. To examine how binocularly asymmetric glaucomatous visual field damage affects binocular disparity processing across the visual field.

Methods. We recruited 18 patients with primary open-angle glaucoma, 16 age-matched controls, and 13 young controls. Participants underwent standard clinical assessments of binocular visual acuity, binocular contrast sensitivity, stereoacuity, and perimetry. We employed a previously validated psychophysical procedure to measure how sensitivity to binocular disparity varied across spatial frequencies and visual field sectors (i.e., with full-field stimuli spanning the central 21° of the visual field and with stimuli restricted to annular regions spanning 0°–3°, 3°–9°, or 9°–21°). We employed measurements with annular stimuli to model different possible scenarios regarding how disparity information is combined across visual field sectors. We adjudicated between potential mechanisms by comparing model predictions to the patterns observed with full-field stimuli.

Results. Perimetry confirmed that patients with glaucoma exhibited binocularly asymmetric visual field damage ($P < 0.001$). Across participant groups, foveal regions preferentially processed disparities at finer spatial scales, whereas periphery regions were tuned for coarser scales ($P < 0.001$). Disparity sensitivity also decreased from fovea to periphery ($P < 0.001$) and across participant groups (Ps < 0.01). Finally, similar to controls, patients with glaucoma exhibited near-optimal disparity integration, specifically at low spatial frequencies ($P < 0.001$).

Conclusions. Contrary to the conventional view that glaucoma spares central vision, we find that glaucomatous damage causes a widespread loss of disparity sensitivity across both foveal and peripheral regions. Despite these losses, cortical integration mechanisms appear to be well preserved, suggesting that patients with glaucoma make the best possible use of their remaining binocular function.

Keywords: glaucoma, binocular disparity, disparity integration mechanisms, visual field loss, binocular function, aging, spatial frequency

Glaucoma is a leading cause of irreversible blindness worldwide, characterized by progressive loss of retinal ganglion cells and resultant visual field defects.[1] The loss and/or dysfunction of retinal ganglion cells often leads to a detrimental effect on various visual functions ranging from simple light detection to complex everyday tasks such as object/face recognition, visual search, reading, and mobility,[2–13] thereby affecting quality of life. Primary open-angle glaucoma, the most common type of glaucoma, is putatively associated with peripheral vision loss. However, there is accumulating evidence that even early glaucomatous injury may involve the macula and that such macular damage may be more common than generally thought.[14–21] For example, a number of anatomic studies[16,19,20,22–26] using spectral-domain optical coherence tomography have shown that the thickness of the retinal nerve fiber layer and the retinal ganglion cell plus inner plexiform layer, even in the macula, is significantly thinner in patients with early glaucoma than in healthy controls. Furthermore, glaucomatous visual field loss often occurs asymmetrically not only between two eyes[27] but also across the visual field.[28] This inhomogeneous nature of glaucomatous visual field deficits is assumed to result in the deterioration of binocular function,[29] which in turn impacts the performance of various everyday visual tasks, such as reading, object recognition, and visuomotor coordination.[30–32] Indeed, studies have shown that, even in early or moderate stages, stereopsis, convergence, and binocular fusion are significantly impaired in people with glaucoma compared to glaucoma suspects or normal cohorts.[33–35]

Human observers extract depth information from binocular disparity (i.e., the differences between retinal images of the two eyes, resulting from the lateral separation of the two eyes). Neurons sensitive to binocular disparities are

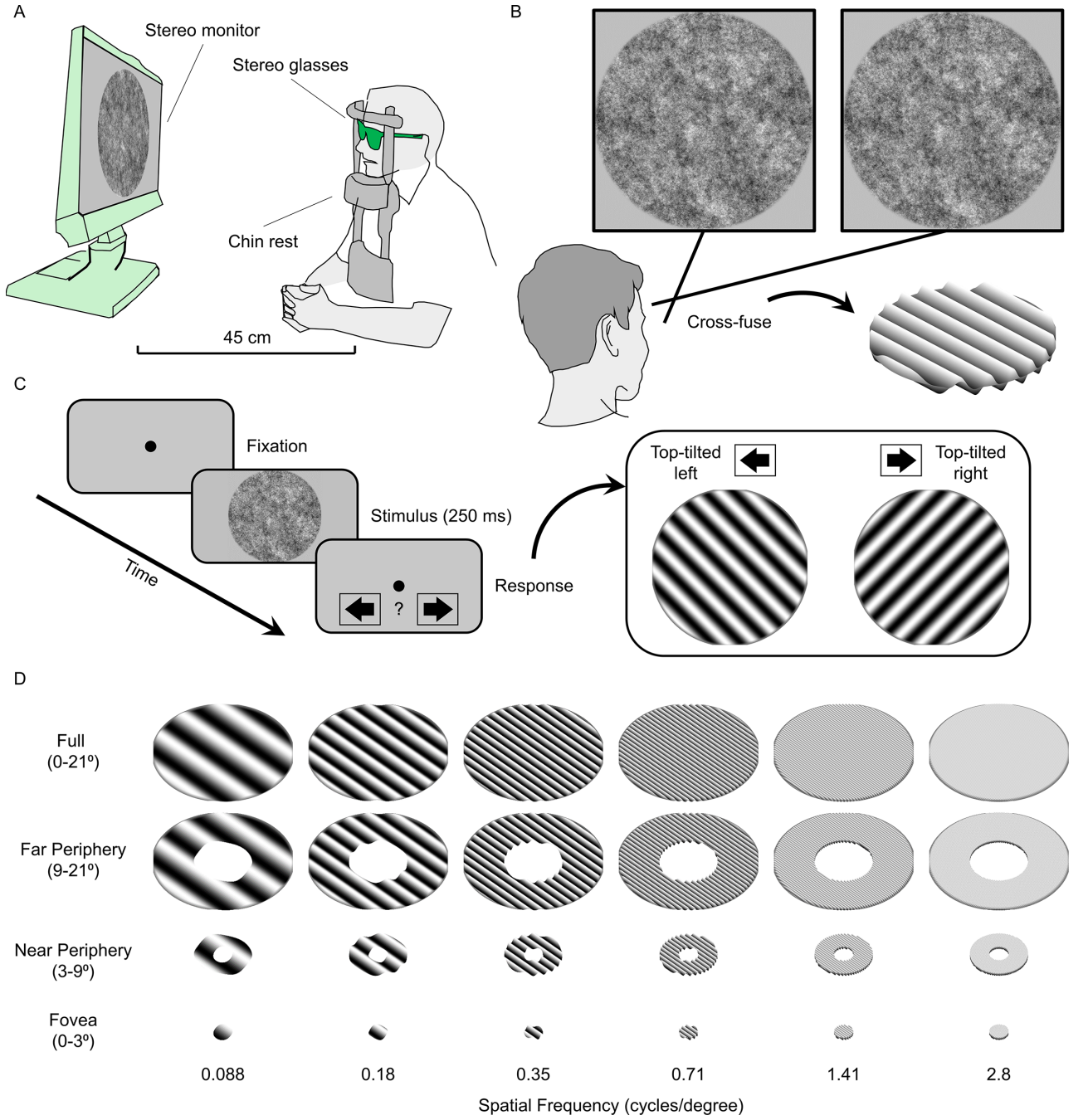

Figure 1. Assessing spatial frequency dependent disparity sensitivity across the visual field. (**A**) Participants seated in front of a stereo monitor viewed dichoptic stimuli through stereo shutter glasses. (**B**) Stimuli were sinusoidal disparity corrugations embedded in pink noise. Cross-fuse the example stimulus pair to view the embedded 3D stimulus. (**C**) On each trial, a stimulus was shown for 250 ms, and participants were asked to report whether the disparity corrugation was top-tilted leftward or rightward. (**D**) Stimuli spanned six spatial frequencies and four visual field conditions.

found in various cortical visual areas,[36] and the perception of disparity-defined depth is a hallmark of binocular visual function. Previous studies in young and healthy normal vision have shown that disparity is processed at different spatial scales in different regions of the visual field[37,38]: the fovea preferentially processes disparities at fine spatial scales, whereas the visual periphery is tuned for coarse spatial scales. Since glaucomatous damage may affect both foveal and peripheral visual field regions asymmetrically in the two eyes, it remains unclear how glaucomatous damage affects disparity sensitivity across the visual field. Moreover, to recover the depth structure of the environment, the healthy visual system selects and combines depth information processed throughout the visual field in near-optimal fashion (i.e., by accounting for the relative reliability of the disparity signals coming from different visual field sectors).[37] However, the question arises as to whether disparity information would be combined in such a near-optimal

manner as shown in normal healthy vision even if disparity signals are asymmetric across the visual field, as expected in glaucomatous vision. In particular, widespread changes in the brain have been shown as a secondary consequence of retinal ganglion cell loss from glaucoma largely due to direct and transsynaptic anterograde degeneration, where ganglion cell damage spreads injury to downstream visual pathways due to loss of presynaptic inputs.[39–41] Therefore, it remains to be seen how glaucomatous damage may affect the visual system's ability to combine depth information throughout the visual field. The objectives of the current study were thus twofold: (1) to elucidate whether disparity sensitivity is visual field dependent in glaucomatous vision and (2) to identify the mechanisms underlying disparity integration across the visual field.

To address the first goal, we measured disparity sensitivity across the visual field of patients with glaucoma and healthy controls using annular pink noise stimuli embedded with disparity corrugations of different spatial scales (i.e., spatial frequencies) and spanning rings of different retinal eccentricities (Fig. 1; a paradigm validated in previous work[37]). Disparity-defined depth corrugations (i.e., sinusoidal disparity gratings) were adopted in the current study as visual sensitivity to disparity corrugations has been shown to be bandpass and eccentricity dependent by nature.[38] Furthermore, disparity corrugations are known to be detected and processed by binocular neurons in the primary visual cortex (V1) and higher visual areas (e.g., middle temporal area MT[42]) that reconstruct the structure of three-dimensional (3D) surfaces.[36] These stimuli thus allow us to study the cortical mechanism underlying disparity integration as well as the global processing of binocular disparities as a function of disparity spatial frequency and eccentricity. In control participants, we expect the tuning of disparity sensitivity to shift from fine to coarse spatial scales as eccentricity increases from the fovea to periphery, as shown in prior studies.[37,38] On the other hand, we envision two different potential scenarios from glaucomatous vision: if glaucomatous damage is predominantly peripheral, we expect impaired disparity sensitivity in peripheral locations and low spatial frequencies; if instead glaucomatous damage involves both foveal and peripheral vision, we expect a uniform loss in disparity sensitivity across visual field locations and spatial frequencies.

To address the second goal, we employed the same data to adjudicate between different potential disparity integration mechanisms. To this end, the disparity sensitivity of each annular condition—representing the sensitivity of each visual field sector—was pitted against that of the full-field condition representing the integrated disparity across the visual field. Specifically, if the visual system is able to appropriately estimate and employ the reliability of binocular disparity signals at different visual field locations, then sensitivity for full-field stimuli should be equal to or better than sensitivity for stimuli spanning smaller areas of the visual field. If instead cortical integration mechanisms fails, we expect performance in the full-field condition to be worse than in the annular conditions. Depending on the extent to which cortical integration mechanisms are altered following glaucomatous damage, different scenarios can thus be speculated and compared[43,44] as follows:

1. **Random selection:** glaucomatous damage may impair cortical integration mechanisms to the point that the system samples disparity information from different visual field locations at random. In this worst-case scenario, disparity sensitivity to full-field stimuli would be much worse than the best sensitivity across visual field locations.
2. **Suboptimal integration:** glaucomatous damage may impair reliability estimates but not cortical integration mechanisms. Without being able to distinguish between visual field locations, disparity signals from all visual field locations would be averaged with equal weight. In this scenario, disparity sensitivity to full-field stimuli would be better than in the random selection case but would still be worse than the best sensitivity across visual field locations.
3. **Optimal selection:** the visual system may be able to estimate the ordinal reliability of disparity signals from different portions of the visual field, meaning which visual field locations contain the most reliable disparity information. If such ordinal information is available, the system could select disparity information from the most reliable visual field regions and discard the rest. In this scenario, disparity sensitivity for full-field stimuli would be equal to the best sensitivity across visual field locations.
4. **(Near-)optimal integration:** the visual system may be able to quantitatively estimate the relative reliability of disparity signals from different regions of the visual field. Disparity information from different visual field locations could thus be weighted by these reliability estimates and combined. If such estimates were accurate, then integration would be optimal (according to the maximum likelihood estimation principle[45–49]), and disparity sensitivity would reach its upper bound. In the more likely scenario that reliability estimates are approximate (i.e., near-optimal integration),[37,50] disparity sensitivity to full-field stimuli would nevertheless be better than the best sensitivity across visual field locations.

In sum, to evaluate the effect of glaucomatous damage and normal aging on the spatial frequency tuning of disparity sensitivity and on the way disparity is integrated across the visual field, we compare outcome measurements between patients with mild to severe glaucoma, age-matched normal controls, and young normal controls. The results of the current study shed light on the nature and inner workings of binocular integration in those with asymmetric visual field loss.

Methods

Participants

We recruited a total of 47 participants for this study: 18 patients with primary open-angle glaucoma (mean age 64 ± 6 years, 7 female), 16 age-matched normally sighted older adults (mean age 61 ± 7 years, 9 female), and 13 normally sighted young adults (mean age 25 ± 4 years, 7 female). Study participants were recruited from either Callahan Eye Hospital Clinics at the University of Alabama at Birmingham (UAB) or the UAB campus. All participants had no known cognitive or neurologic impairments, further confirmed by the Mini Mental State Examination (score ≥ 25 for those aged 65 and over). Participants were fitted with proper refractive correction for the viewing distance throughout the study. Patients with glaucoma, whose diagnosis was

validated through medical records, met the following inclusion criteria:

(i) Glaucoma-specific changes of optic nerve or nerve fiber layer defect: the presence of the glaucomatous optic nerve was defined by masked review of optic nerve head photos by glaucoma specialists using previously published criteria.[51]
(ii) Glaucoma-specific visual field defect: a value of the Glaucoma Hemifield Test from the Humphrey Field Analyzer (HFA) outside normal limits.
(iii) No history of other ocular or neurologic disease or surgery that caused visual field loss.

All experimental protocols followed the tenets of the sixth revision of the Declaration of Helsinki (2008) and were approved by the Internal Review Board at UAB. We obtained written informed consent from all participants prior to the experiment, after having explained to them the nature of the study.

Clinical Assessments of Binocular Visual Function

We assessed binocular visual function in patients and controls through standard clinical measures of binocular visual acuity (Early Treatment Diabetic Retinopathy Study charts), binocular contrast sensitivity (Pelli-Robson charts), and stereoacuity (Titmus Fly SO-001 StereoTest). We report visual acuity in logMAR, contrast sensitivity in log units (logCS), and stereoacuity in seconds of arc (arcsec). We further assessed visual field sensitivities in both eyes (24-2 test with a Humphrey Field Analyzer; Carl Zeiss Meditec, Inc., Jena, Germany) and recorded the mean deviation value obtained from the HFA 24-2 test, which is commonly used for evaluating the severity of glaucoma. The Table reports the characteristics of study participants. According to the Hodapp–Anderson–Parish glaucoma grading system,[52] most of our patients were in early to moderate stages of glaucoma (13 of 18).

Measuring Disparity Sensitivity

We adopted a previously published experimental paradigm[37] to measure the spatial frequency tuning of disparity sensitivity across different regions of the visual field.

Stimuli and Apparatus. Stimuli and experimental procedures were generated and controlled using MATLAB (version 8.3; The MathWorks, Inc., Natick, MA, USA) and Psychophysics Toolbox extensions (version 3)[53,54] in Windows 7, running on a PC desktop computer (model: Dell Precision Tower 5810). Stimuli were presented on a liquid crystal display monitor (model: Asus VG278HE; refresh rate: 144 Hz; resolution: 1920 × 1080; dot pitch 0.311 mm) with the mean luminance of the monitor at 159 cd/m^2. The luminance of the display monitor was linearized using an 8-bit lookup table in conjunction with photometric readings from a Minolta LS-110 luminance meter (Konica Minolta, Inc., Tokyo, Japan). Participants were seated in a dimly lit room, 45 cm in front of the monitor with their heads stabilized in a chin and forehead rest, and wore active stereoscopic shutter-glasses (NVIDIA 3DVision, NVIDIA, Santa Clara, California, USA) to control dichoptic stimulus presentation (Fig. 1A). The crosstalk of the dichoptic system was 1% measured with a Spectrascan 6500 photometer (Photo Research, Chatsworth, CA, USA). Stimuli were 1/f pink noise stereograms presented on a uniformly gray background (Fig. 1B). Stimuli were presented as disks or rings with 1° cosinusoidal edges and contained oblique (±45° from vertical) sinusoidal disparity corrugations of varying amplitude and spatial frequency (generated as in Maiello et al.[37] and Reynaud et al.[55]; see also Georgeson et al.[56]). The central fixation target was a 0.25° black disk with 0.125° cosinusoidal edge.

Procedure. On each trial (Fig. 1C), observers were presented with a black fixation dot on a uniformly gray background. As soon as the response from the previous trial had been recorded, the stimulus for the current trial was shown for 250 ms. This was too brief a presentation time for participants to benefit from changes in fixation, since stimulus-driven saccade latencies are typically greater than 200 ms,[57] saccade durations range from 20 to 200 ms,[58] and visual sensitivity is reduced during and after a saccade.[59,60] Once a stimulus had been extinguished, participants were asked to indicate, via button press, whether the disparity corrugation was top-tilted leftward or rightward. Participants were given unlimited time to respond, and the following trial commenced as soon as a response was provided. On each trial, we modulated the amount of peak-to-trough disparity under the control of a three-down, one-up staircase[61] that adjusted the disparity magnitude to a level that produced 79% correct responses.

Design. We measured how each participant's disparity sensitivity (1/disparity threshold) varied, as a function of the spatial frequency of the sinusoidal disparity corrugation, throughout different portions of the visual field. Specifically, we measured disparity thresholds at six spatial frequencies (0.088, 0.18, 0.35, 0.71, 1.41, and 2.8 cycles/degree) and across four visual field conditions (Fig. 1D). In the full visual field condition, stimuli were presented within a disk with a 21° radius centered at fixation. In the far and near peripheral visual field conditions, stimuli were presented within rings spanning 9° to 21° and 3° to 9° into the visual periphery, respectively. Finally, in a foveal condition, stimuli were presented within a disk with a 3° radius. We measured disparity thresholds for each combination of spatial frequency and visual field condition via 24 randomly interleaved staircases.[61] We combined the raw data from 50 trials from each staircase and fitted these data to a cumulative normal function via weighted least squares regression (in which the data are weighted by their binomial standard deviation). We then computed disparity discrimination thresholds from the 75% correct point of the fitted psychometric functions. We converted thresholds into disparity sensitivity following the relationship: sensitivity = 1/threshold.

Spatial Frequency Tuning Across The Visual Field. Disparity sensitivity is known to vary lawfully as a function of spatial frequency following an inverted-U shape[62,63] that is well captured by a three-parameter log-parabola disparity sensitivity function (DSF) model defined as follows[37,55]:

$$DSF(f) = \log_{10}(\gamma_{max}) - \log_{10}(2)\left(\frac{\log_{10}(f) - \log_{10}(f_{max})}{\log_{10}(2\beta)/2}\right)^2$$

In this equation, γ_{max} represents the peak gain (i.e., peak sensitivity), f_{max} is the peak frequency (i.e., the spatial frequency at which the peak gain occurs), and β is the bandwidth at half-height (in octaves) of the function. We

Table. Characteristics of Study Participants

Diagnosis	Age, y	Sex	Binocular Visual Acuity (logMAR)	Binocular Contrast Sensitivity (logCS)	Stereoacuity (arcsec)	HFA 24-2 Mean Deviation (dB)	
						OD	OS
POAG	62	F	0.02	1.5	80	−15.58	−6.51
POAG	63	M	0.02	1.65	40	−0.61	−2.39
POAG	68	F	−0.08	NA	40	−0.28	0.81
POAG	74	F	0.04	1.65	40	−1.91	−15
POAG	62	M	0.12	1.65	100	−9.55	−10.63
POAG	67	M	−0.1	1.95	40	1.54	0.58
POAG	56	M	−0.02	1.5	50	−20.91	−27.88
POAG	73	M	−0.1	1.35	400	−23.65	−23.9
POAG	65	M	0.02	1.65	50	−2.38	−15.66
POAG	64	M	0	1.95	40	−0.71	−1.71
POAG	73	M	0.06	1.65	50	−5.94	−6.94
POAG	59	F	0.04	1.65	50	−1.06	−1.75
POAG	60	F	−0.12	1.9	40	1.16	−0.55
POAG	62	M	−0.1	1.9	40	−2.42	−4.64
POAG	68	M	0.04	1.7	100	0	−7.63
POAG	59	F	0.04	2.1	40	−0.3	1.01
POAG	55	F	−0.06	1.75	40	−4.25	−7.7
POAG	60	M	0.04	1.7	100	−1.02	−6.57
AMC	51	M	−0.2	2.1	40	1.6	0.99
AMC	55	M	−0.18	1.95	40	1.98	1.99
AMC	65	M	−0.12	1.95	40	0.74	−0.87
AMC	63	M	−0.08	1.95	50	0	−0.24
AMC	61	M	−0.2	2.1	40	−1.58	1.35
AMC	65	M	−0.04	1.95	100	−0.08	−0.73
AMC	63	F	−0.02	1.95	40	−1.11	0.01
AMC	67	F	0.02	1.95	40	−1.3	−1.75
AMC	70	F	−0.02	1.95	60	−0.39	−2.41
AMC	56	F	−0.08	1.9	60	3.12	2.05
AMC	62	F	−0.14	1.95	40	2.6	1.07
AMC	50	F	−0.02	1.95	40	−0.93	0.59
AMC	69	F	−0.06	1.95	40	−0.13	1.59
AMC	51	F	−0.2	2.1	40	0.31	1.83
AMC	65	M	0.02	1.8	50	−1.14	0.9
AMC	57	F	−0.18	1.95	40	2.15	1.06
YC	27	M	−0.18	1.9	40	−0.81	−0.85
YC	25	F	−0.22	2.1	40	1.02	1.2
YC	31	F	−0.12	2.15	40	NA	NA
YC	23	F	−0.18	2	40	0.19	−1.25
YC	26	M	−0.24	2.25	40	0.87	1.16
YC	24	F	−0.2	2.25	40	NA	NA
YC	34	M	−0.18	1.95	40	1.06	0.4
YC	26	M	−0.06	1.95	40	0.35	−0.17
YC	25	F	−0.2	2.1	50	NA	NA
YC	22	F	−0.12	1.95	40	1.01	−1.58
YC	20	M	−0.016	1.95	40	−2.12	−1.89
YC	20	F	−0.2	1.8	40	−0.25	−0.9
YC	21	M	−0.02	1.95	40	−0.53	−1.62

AMC, age-matched control; logCS, contrast sensitivity in log units; NA, not available; OD, right eye; OS, left eye; POAG, primary open-angle glaucoma; YC, young control.

thus fit the disparity sensitivity data to this equation separately for each visual field condition, obtaining parameter estimates that we then compared across visual field conditions and participant groups. In the full-field condition, we further computed the area under the log DSF (AULDSF) as an additional estimate of binocular function across participants.

Disparity Integration Models. Following established theories and formulations of sensory cue integration,[43] we defined four possible models of disparity integration across the visual field:

1. **Random selection**, in which disparity information is sampled from different visual field locations at random. To model this worst-case scenario, disparity thresholds to full-field stimuli were estimated from the restricted visual field conditions as

$$T_{FF-Rand} = \sqrt{\frac{T_{0-3}^2 + T_{3-9}^2 + T_{9-21}^2}{3}}$$

2. **Suboptimal integration**, in which disparity information is averaged from all visual field locations with equal weight. To model this scenario, disparity thresholds to full-field stimuli were estimated as

$$T_{FF-SubOpt} = \sqrt{\frac{\left(\frac{T_{0-3}^2+T_{3-9}^2+T_{9-21}^2}{3}\right)^3}{3 \times \left(\frac{T_{0-3}^2+T_{3-9}^2+T_{9-21}^2}{3}\right)^2}}$$

3. **Optimal selection**, in which disparity information is sampled only from the most reliable region of the visual field. To model this scenario, disparity thresholds to full-field stimuli were estimated as

$$T_{FF-OptSel} = min\left(T_{0-3},\ T_{3-9}, T_{9-21}\right)$$

4. **Optimal integration**, in which disparity signals from different visual field locations are averaged, weighted by their relative reliability. To model this scenario, which represents the theoretical upper bound of performance, disparity thresholds to full-field stimuli were estimated as

$$T_{FF-OptInt} = \sqrt{\frac{T_{0-3}^2 T_{3-9}^2 T_{9-21}^2}{T_{0-3}^2 T_{3-9}^2 + T_{0-3}^2 T_{9-21}^2 + T_{3-9}^2 T_{9-21}^2}}$$

Statistical Analyses

Sample Size Selection. Comparisons of binocular visual function between patients with glaucoma and controls typically yield very large effect sizes (e.g., Bassi and Galanis[33]; Cohen's $d > 2$). Effect sizes for within-participant effects of interest are similarly large (e.g., Maiello et al.[37]; Cohen's $d > 1$). Given that we were interested in detecting substantial effects of potential clinical significance, we exceeded a minimum sample size of $N = 10$ per participant group. This ensured we would surpass 80% power at the 0.05 significance level for detecting effect sizes of $d = 1$ for both between- and within-group comparisons. We report effect sizes for all comparisons performed in the study in terms of either Cohen's d or η^2, as appropriate.

Between-Group Comparisons of Binocular Visual Function. We expected binocular visual function to be worse in old compared to young adults and in patients with glaucoma compared to both young and old healthy controls. We tested for these expected differences using one-tailed *t*-tests (for normally distributed data) or Wilcoxon rank-sum tests (for skewed data).

Comparison of Spatial Frequency Tuning Across Participant Groups and Visual Field Conditions. To test whether disparity tuning to spatial frequency varied across the participants' visual field and across participant groups, we analyzed DSF parameter estimates from the restricted visual field conditions using a 3 (participant group, between-subjects factor) × 3 (visual field condition, within-subject factor) mixed-model ANOVA. ANOVA normality assumptions were verified via quantile–quantile plots. When appropriate, we conducted post hoc comparisons via two-tailed *t*-tests.

Model Selection. To adjudicate which candidate disparity integration model best accounted for the full-field data at each spatial frequency and in each participant group, we employed a simple model selection rule. Specifically, we selected as the best-fitting model the one that minimized the root mean square error to the full-field data. If the optimal integration model won, we further confirmed whether full-field sensitivities significantly differed from the optimal selection model, using one-tailed *t*-tests. This was necessary to validate that full-field sensitivity truly reflected near-optimal integration. We excluded from these analyses participants whose median disparity thresholds across spatial frequency and visual field conditions were greater than 10 minutes of arc. Above this threshold, participants are either stereo blind or not reliably performing the task,[37] and we reasoned that it would be uninformative to assess disparity integration in these participants. Based on this criterion, we thus excluded four patients with glaucoma, one age-matched control participant, and one young control participant.

Results

Glaucoma and Normal Aging Exhibit Expected Patterns of Binocular Visual Impairment

We evaluated binocular visual function in patients and controls using standard clinical assessment tools as described in the Methods. As expected, binocular visual acuity (Fig. 2A) was worse in old compared to young participants ($t(27) = 1.9$, $P = 0.035$; $d = .7$) and in patients with glaucoma compared to both young ($t(29) = 5.4$, $P < 0.001$; $d = 2$) and age-matched ($t(32) = 3.3$, $P = 0.0011$; $d = 1.1$) control participants. Binocular contrast sensitivity (Fig. 2B) was not significantly different between old and young control participants ($t(27) = 1.4$, $P = 0.082$; $d = .53$) but was significantly impaired in patients with glaucoma compared to both young ($t(28) = 4.9$, $P < 0.001$; $d = 1.8$) and age-matched controls ($t(31) = 4.8$, $P < 0.001$; $d = 1.7$). Stereoacuity (Fig. 2C) was significantly worse in patients with glaucoma compared to young ($z = 2.5$, $P = 0.0064$; $d = 0.52$) but not age-matched controls ($z = -1.2$, $P = 0.12$; $d = .43$), and the difference between old and young control participants did not reach statistical significance ($z = -1.6$, $P = 0.057$; $d = .57$). Finally, we visualized the mean deviation values from the HFA 24-2 test in participants' better versus worse eyes (Fig. 2D). The difference in HFA 24-2 mean deviation across the two eyes was much greater in patients with glaucoma compared to both young ($t(26) = 3.5$, $P < 0.001$; $d = 1.4$) and age-matched controls ($t(32) = -2.7$, $P = 0.0050$; $d = .94$), whereas young and old control participants exhibited similar interocular differences in HFA 24-2 mean deviation ($t(24) = 0.56$, $P = 0.29$; $d = .23$). Together, these results clearly indicate that patients with glaucoma exhibited substantial binocular visual impairment that was due specifically to asymmetric patterns of visual field loss across the two eyes.

Glaucoma Exhibits Uniform Loss in Disparity Sensitivity Across Spatial Frequencies and Visual Field Locations

Having verified that our patient cohort exhibited interocularly asymmetric glaucomatous visual field loss, we proceeded to test how this impacted disparity processing. When tested with full-field stimuli extending from the fovea to 21° into the visual periphery (Fig. 3A), patients with glaucoma exhibited a uniform loss of disparity sensitivity across spatial frequencies compared to control participants,

Investigative Ophthalmology & Visual Science

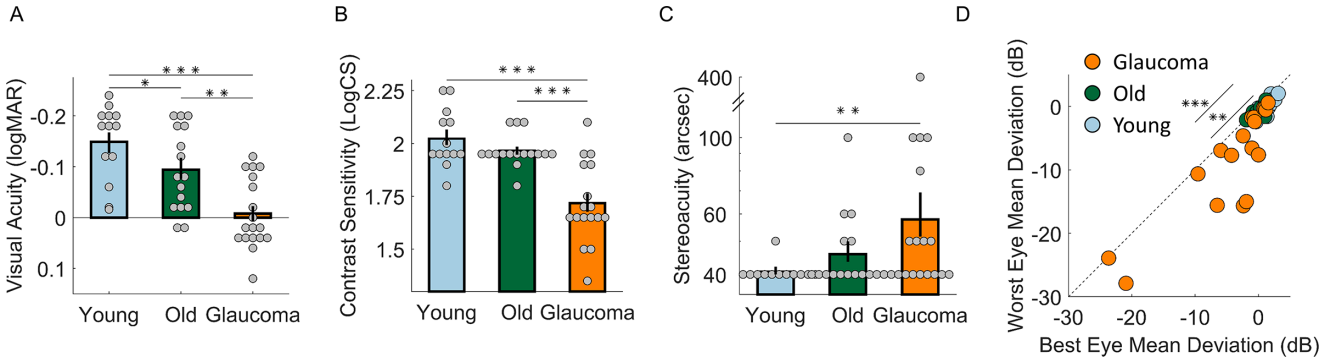

Figure 2. Binocular visual function in patients with glaucoma and control participants. Binocular visual acuity (**A**), binocular contrast sensitivity (**B**), and stereoacuity (**C**) in patients and controls. (**D**) Scatterplot of Humphrey 24-2 visual field mean deviation in better versus worse eye. The *black dotted line* indicates the identity line where the mean deviation of the better eye is equal to that of the worse eye. Across panels, *bars* are means, *error bars* represent bootstrapped standard error of the mean, and *dots* represent data from individual participants. $^{*}P < 0.5$. $^{**}P < 0.01$. $^{***}P < 0.001$.

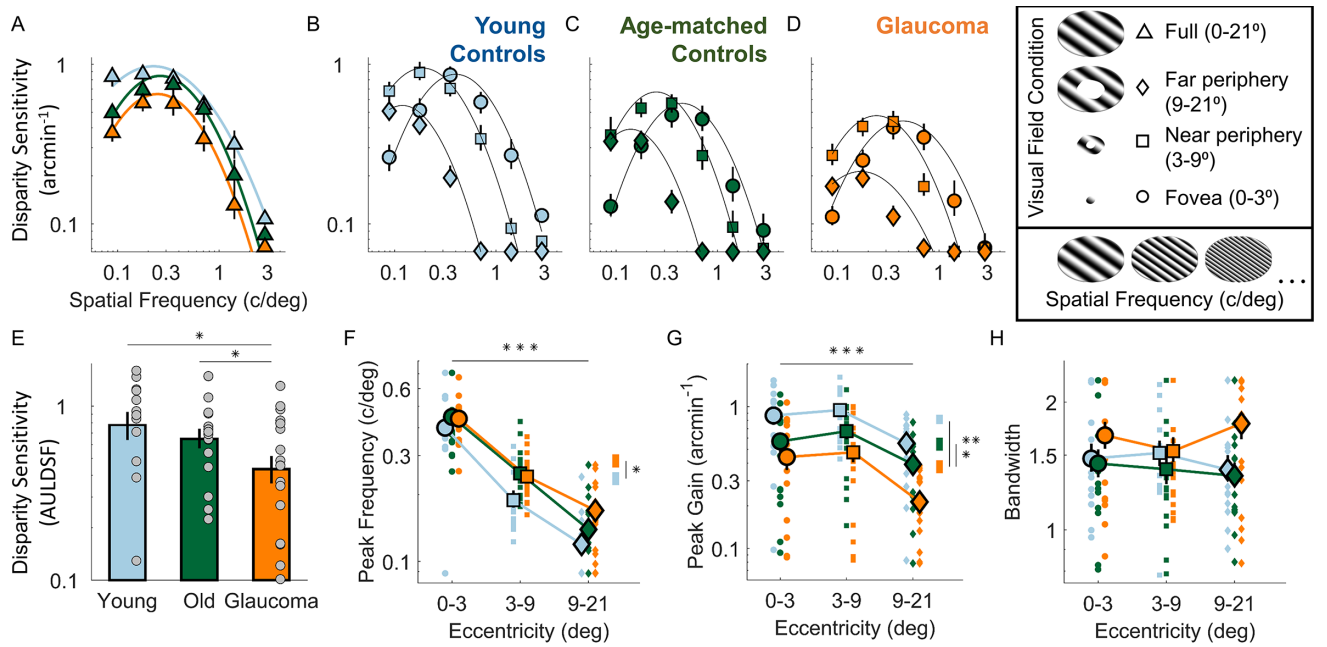

Figure 3. Disparity sensitivity across the visual field. (**A**) Disparity sensitivity plotted as a function of spatial frequency for full-field stimuli in patients and controls. (**B–D**) Disparity sensitivity as a function of spatial frequency for stimuli spanning far (*diamonds*), near (*squares*), and foveal (*circles*) portions of the visual field, plotted separately for young controls (**B**), age-matched controls (**C**), and patients with glaucoma (**D**). In **A–D**, continuous lines are the average best-fitting log parabola functions passing through the data. (**E**) Area under the log disparity sensitivity function for full-field stimuli in patients and controls. (**F–H**) Peak frequency (**F**), peak gain (**G**), and bandwidth (**H**) of the fitted log parabola models as a function of the portion of visual field tested in patients and controls. Across panels, *bars* and *large markers* are means, *dots* and *small markers* represent data from individual participants, and *error bars* and *shaded regions* represent bootstrapped standard error of the mean. $^{*}P < 0.5$. $^{**}P < 0.01$. $^{***}P < 0.001$.

suggesting glaucomatous damage is implicated in both the central and peripheral visual field. Indeed, the AULDSF fitted to the full-field condition (Fig. 3E) was significantly reduced in patients with glaucoma compared to both young ($t(29) = 2.2$, $P = 0.018$; $d = .8$) and age-matched ($t(32) = 1.7$, $P = 0.048$; $d = .59$) controls, whereas sensitivity did not significantly differ between young and old control groups ($t(27) = 0.81$, $P = 0.21$; $d = .3$). Further, when tested with stimuli spanning restricted portions of the visual field (Figs. 3B–D), patients with glaucoma exhibited a uniform loss of disparity sensitivity also across the visual field. In all three participant groups, the spatial frequency tuning of disparity sensitivity varied similarly across different regions of the visual field. As expected, disparity sensitivity in the far periphery (diamond markers) was tuned to depth variations at low spatial frequencies, disparity sensitivity in the near periphery (square markers) was tuned to mid spatial frequencies, and disparity sensitivity at the fovea (circle markers) was tuned to high spatial frequencies. Figures 3F–H further summarize these shifts across participant groups. Specifically, the peak frequency of the disparity sensitivity curves (Fig. 3F) shifted from high to low frequencies from the fovea to the peripheral visual field (visual field main effect: $F_{2,\ 88} = 260$, $P < .001$; $\eta^2 = .64$). ANOVA results further revealed a

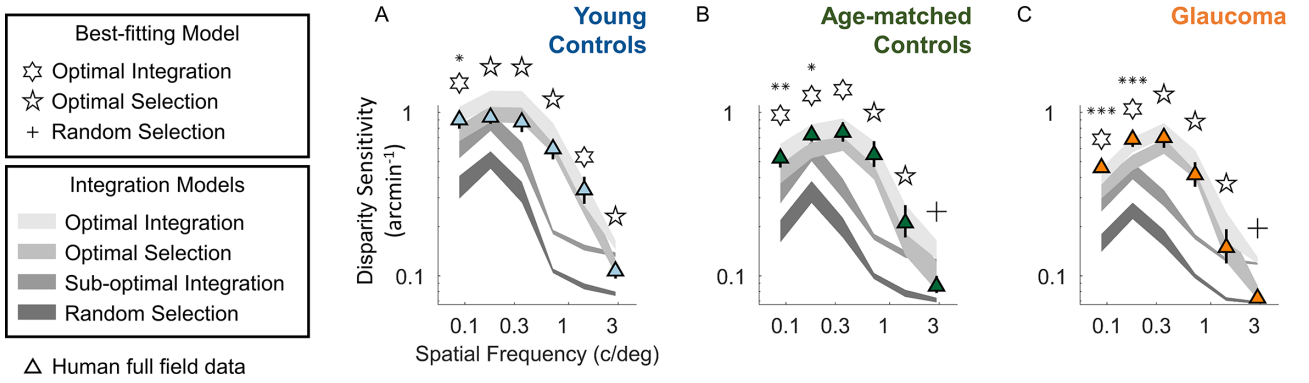

Figure 4. Disparity integration across the visual field: model selection and comparison. (**A–C**) Model predictions and psychophysical measurements of disparity sensitivity for full-field stimuli, plotted as a function of spatial frequency for young controls (**A**), age-matched controls (**B**), and patients with glaucoma (**C**). *Triangle markers* indicate mean values across participants, and *error bars* and *shaded regions* represent bootstrapped standard error of the mean. *$P < 0.5$. **$P < 0.01$. ***$P < 0.001$.

main effect of participant group ($F_{2, 44} = 3.5$, $P = 0.039$; $\eta^2 = .033$) but no interaction between visual field and participant group factors ($F_{4, 88} = 1.2$, $P = 0.31$; $\eta^2 = .006$). Post hoc tests revealed a uniform shift toward higher spatial frequencies in patients with glaucoma compared to young ($t(29) = 2.6$, $P = 0.014$; $d = .95$) but not age-matched controls ($t(32) = .63$, $P = 0.53$; $d = .22$) and no significant difference between young and old participants ($t(27) = 1.8$, $P = 0.076$; $d = .69$). The peak gain of the disparity sensitivity curves (Fig. 3G) also decreased —as expected —from the fovea to the peripheral visual field (visual field main effect: $F_{2, 88} = 28$, $P < 0.001$; $\eta^2 = .097$) and varied across participant groups ($F_{2, 44} = 7.1$, $P = 0.0021$; $\eta^2 = .18$), uniformly (visual field × participant group interaction effect: $F_{4, 88} = .35$, $P = 0.84$; $\eta^2 = .0024$). Post hoc tests revealed that patients with glaucoma had significantly reduced peak gain compared to both young ($t(29) = 3.7$, $P = 0.001$; $d = 1.3$) and age-matched controls ($t(32) = 2.1$, $P = 0.047$; $d = .71$), whereas the difference between old and young participants was not statistically significant ($t(27) = 1.8$, $P = 0.082$; $d = .67$). Finally, the bandwidth of disparity tuning (Fig. 3H) remained constant across visual field locations and patient groups (visual field main effect: $F_{2, 88} = .11$, $P = 0.9$; $\eta^2 = .001$; participant group main effect: $F_{2, 44} = 2.7$, $P = 0.081$; $\eta^2 = .061$; visual field × participant group interaction effect: $F_{4, 88} = .88$, $P = 0.48$; $\eta^2 = .017$). These patterns confirmed previous reports regarding the tuning of human disparity sensitivity across different regions of the visual field.[37] More important, and contrary to the commonly held belief that early glaucomatous damage is predominantly peripheral, these results demonstrated that patients with glaucoma had a uniform loss of disparity sensitivity across both foveal and peripheral visual sectors.

All Groups Exhibit Near-Optimal Disparity Integration Across The Visual Field

Our results thus far determined that interocularly asymmetric glaucomatous visual field loss leads to impaired disparity sensitivity both foveally and peripherally, as well as across spatial frequencies. Does this in turn impair the way disparity signals are integrated across the visual field? To test this, we used the sensitivity data from the restricted visual field conditions to generate predictions for full-field sensitivities in four possible scenarios: random selection, suboptimal integration, optimal selection, and optimal integration, as described earlier. Across all three participant groups (Figs. 4A–C) and across nearly all spatial frequencies, full-field sensitivity data approached the upper bounds of possible performance and were best fit by either the optimal selection or optimal integration models. Furthermore, full-field sensitivities were significantly better than the optimal selection model—and thus conclusively reflected near-optimal integration—predominantly at low spatial frequencies. Specifically, disparity integration was significantly near optimal at the lowest spatial frequency tested in young participants (Fig. 4A, 0.088 cycles/degree: $t(11) = 2.6$, $P = 0.013$; $d = .74$), age-matched controls (Fig. 4B, 0.088 cycles/degree: $t(14) = 3.1$, $P = 0.0039$; $d = .8$), and patients with glaucoma (Fig. 4C, 0.088 cycles/degree: $t(13) = 4$, $P < 0.001$; $d = 1.1$). Performance was also significantly near optimal at the second lowest spatial frequency tested in both age-matched controls (Fig. 4B, 0.18 cycles/degree: $t(14) = 2.4$, $P = 0.015$; $d = .62$) and patients with glaucoma (Fig. 4C, 0.18 cycles/degree: $t(13) = 6.1$, $P < 0.001$; $d = 1.6$). These results indicate that participants reliably integrated low-spatial frequency disparity information most clearly across far- and mid-peripheral visual field sectors. At higher spatial frequencies instead, participants may have relied more dominantly on foveal disparity estimates. Critically, even though patients with glaucoma exhibited significant asymmetric visual field defects and impairments in disparity processing, cortical mechanism for disparity integration appeared to be spared.

Discussion

Binocular disparity is a key component of depth perception. In healthy humans, foveal regions preferentially process disparities at fine spatial scales, peripheral visual regions are tuned for coarse spatial scales, and the visual cortex selects and combines depth information across different visual regions by accounting for these differences in tuning.[37] Glaucoma is a neurodegenerative condition characterized by progressive loss of retinal ganglion cells and resulting visual field defects. Even in early stages of the disease, glaucomatous ganglion cell damage results in patterns of visual sensitivity loss that may vary both across the visual

field and between the eyes.[15,19,27,64] Additionally, damage to ganglion cells can potentially propagate to cortical regions due to direct and transsynaptic anterograde axonal degeneration.[39–41] For this reason, it is highly plausible that glaucoma could lead to impairments in binocular disparity processing across the visual field and even along the cortical visual processing pathway. Thus, here we assessed how glaucomatous visual field damage impacted spatial frequency–dependent disparity sensitivity across different sectors of the visual field.

Using a previously validated experimental paradigm,[37] we assessed the spatial frequency–dependent disparity sensitivity across the visual field and further determined the best integration model accounting for the full-field disparity sensitivity data of glaucomatous vision. Our results demonstrate several fundamental aspects of glaucomatous visual loss. First, we observed a uniform loss in disparity sensitivity across visual field locations and spatial frequencies in glaucoma, compared to both young and age-matched healthy controls. This demonstrates that foveal vision and binocular function are impacted even in early glaucoma. Second, we found that disparity sensitivity to full-field stimuli was equal to or better than sensitivity for stimuli spanning smaller areas of the visual field, in glaucoma and control patients alike. The glaucomatous visual system is thus able to access—at least to some extent—the reliability of the signals coming from different regions of its damaged visual field. Further, early glaucomatous loss does not substantially impact cortical selection and integration mechanisms, leading to near-optimal processing of binocular disparity even given the presence of binocularly asymmetric glaucomatous lesions across the visual field.

Previous studies have reported that binocular function, including stereopsis, is significantly impaired in glaucomatous vision.[27,33] However, glaucomatous stereovision deficits have been characterized almost exclusively in terms of stereoacuity, and such deficits have been identified even in glaucoma suspects.[35] This is perhaps surprising, given how glaucomatous damage is believed to spare the central vision until the end stages of the disease, whereas stereoacuity refers to fine spatial scales that should be processed at the fovea. Our results reconcile this apparent contradiction by demonstrating that patients with glaucoma exhibit a loss of disparity sensitivity across spatial scales, from the fovea to the visual periphery. Furthermore, our findings lend strength to the view that macular damage may commonly occur even in early stages of glaucoma.[14–21]

The observed glaucomatous deficits in stereovision across the visual field could have affected cortical processing in several ways. In the most extreme scenario, glaucomatous neurodegeneration could have propagated from retinal regions upward along the visual pathway,[39–41] reaching cortical regions responsible for selecting and combining disparity depth information across the visual field. Alternatively, even if cortical integration mechanisms had been spared, glaucomatous damage could have unpredictably altered the reliability of disparity signals across the visual field, rendering integration processes suboptimal. Instead, our analyses revealed that patients with glaucoma performed near-optimal integration of disparity information across visual field sectors, particularly at coarse spatial scales preferentially processed across peripheral visual regions. This finding is far from trivial, since patients with glaucoma are often unaware of the localization of their visual field deficits, particularly when these are asymmetric between the eyes.[65,66] It is thus notable that the visual system can appropriately select disparity information from different visual field sectors and even combine this information, weighted by the relative reliability of the disparity signals. This suggests not only that cortical disparity integration mechanisms are spared but that —at least in early or moderate stages of the disease —the system is able to adapt and make the best possible use of the remaining binocular visual function. Our findings are indeed consistent with previous work[67] demonstrating that the mechanism underlying the binocular summation of contrast sensitivity (i.e., a quadratic summation rule with an exponent of 1.3) remains well preserved even in patients with early and moderate glaucoma. Taken together, cortical binocular integration mechanisms, whether the signal is luminance contrast or disparity, appear to be spared in glaucomatous vision despite binocularly asymmetric vision loss.

While such findings hint at potential treatment opportunities for preserving or restoring binocular function[32,68–72] in early or moderate glaucoma, we acknowledge that whether this would occur also in more advanced disease stages needs to be addressed in future studies. Further, the stimuli employed here are relatively simple, corrugated 3D surfaces. In the natural world, however, disparity is inhomogeneous: both healthy humans and patients with glaucoma experience natural and unnatural variations in disparity throughout the visual field that they must integrate into a single, rich naturalistic percept. Future research should thus assess whether our current findings with controlled stimuli extend to naturally occurring patterns of retinal disparities. In addition, it may be feasible to perform more quantitative assessments[25,37,73,74] of the relationship between the pattern of glaucomatous visual field defects and the pattern of impairment in disparity processing. For example, it should be possible to map out the monocular impairments of individual patients through perimetry and then use these maps to simulate visual field impairments in both healthy observers and computational models of disparity processing.[37] If glaucomatous damage is indeed limited to the retina and does not affect cortical processing, we would expect that simulated lesions should be sufficient to re-create the patterns of disparity sensitivity loss experienced by individual patients with glaucoma. If successful, such an approach would help to further characterize glaucomatous injury and potentially even tailor treatment strategies to individual patients.

Acknowledgments

The authors thank Marguerite Devereux, Rong Liu, and Lindsay Washington for their help with subject recruitment and data collection.

Supported by the DFG (German Research Foundation: project No. 222641018-SFB/TRR 135 TP C1), NIH/NEI Grant R01 EY027857, and Research to Prevent Blindness (RPB)/Lions' Clubs International Foundation (LCIF) Low Vision Research Award.

The funding organizations had no role in the design or conduct of this research.

Data and analysis scripts are available from the Zenodo database (doi:10.5281/zenodo.7802555).

Disclosure: **G. Maiello**, None; **M.Y. Kwon**, None

References

1. Friedman DS, Wolfs RCW, O'Colmain BJ, et al. Prevalence of open-angle glaucoma among adults in the United States. *Arch Ophthalmol*. 2004;122(4):532–538.
2. Mathews PM, Rubin GS, McCloskey M, Salek S, Ramulu PY. Severity of vision loss interacts with word-specific features to impact out-loud reading in glaucoma. *Invest Ophthalmol Vis Sci*. 2015;56(3):1537–1545.
3. Ramulu PY, Swenor BK, Jefferys JL, Friedman DS, Rubin GS. Difficulty with out-loud and silent reading in glaucoma. *Invest Ophthalmol Vis Sci*. 2013;54(1):666.
4. Nguyen AM, van Landingham SW, Massof RW, Rubin GS, Ramulu PY. Reading ability and reading engagement in older adults with glaucoma. *Invest Ophthalmol Vis Sci*. 2014;55(8):5284.
5. Glen FC, Crabb DP, Smith ND, Burton R, Garway-Heath DF. Do patients with glaucoma have difficulty recognizing faces? *Invest Ophthalmol Vis Sci*. 2012;53(7):3629.
6. Kwon M, Liu R, Patel BN, Girkin C. Slow reading in glaucoma: Is it due to the shrinking visual span in central vision? *Invest Ophthalmol Vis Sci*. 2017;58(13):5810.
7. Chien L, Liu R, Girkin C, Kwon M. Higher contrast requirement for letter recognition and macular RGC+ layer thinning in glaucoma patients and older adults. *Invest Ophthalmol Vis Sci*. 2017;58(14):6221.
8. JY E, Mihailovic A, Garzon C, et al. Association between visual field damage and gait dysfunction in patients with glaucoma. *JAMA Ophthalmol*. 2021;139(10):1053.
9. Kotecha A, O'Leary N, Melmoth D, Grant S, Crabb DP. The functional consequences of glaucoma for eye–hand coordination. *Invest Ophthalmol Vis Sci*. 2009;50(1):203.
10. Smith ND, Crabb DP, Garway-Heath DF. An exploratory study of visual search performance in glaucoma: Study of visual search performance in glaucoma. *Ophthalmic Physiol Opt*. 2011;31(3):225–232.
11. Wiecek E, Pasquale LR, Fiser J, Dakin S, Bex PJ. Effects of peripheral visual field loss on eye movements during visual search. *Front Psychology*. 2012;3:472.
12. Kwon M, Huisingh C, Rhodes LA, McGwin G, Wood JM, Owsley C. Association between Glaucoma and at-fault motor vehicle collision involvement among older drivers. *Ophthalmology*. 2016;123(1):109–116.
13. McGwin G, Xie A, Mays A, et al. Visual field defects and the risk of motor vehicle collisions among patients with glaucoma. *Invest Ophthalmol Vis Sci*. 2005;46(12):4437.
14. Quigley HA, Addicks EM, Green WR. Optic nerve damage in human glaucoma. III. Quantitative correlation of nerve fiber loss and visual field defect in glaucoma, ischemic neuropathy, papilledema, and toxic neuropathy. *Arch Ophthalmol*. 1982;100(1):135–146.
15. Elze T, Pasquale LR, Shen LQ, Chen TC, Wiggs JL, Bex PJ. Patterns of functional vision loss in glaucoma determined with archetypal analysis. *J R Soc Interface*. 2015;12(103):20141118.
16. Hood DC, Raza AS, de Moraes CGV, Liebmann JM, Ritch R. Glaucomatous damage of the macula. *Prog Retin Eye Res*. 2013;32:1–21.
17. Medeiros FA, Lisboa R, Weinreb RN, Liebmann JM, Girkin C, Zangwill LM. Retinal ganglion cell count estimates associated with early development of visual field defects in glaucoma. *Ophthalmology*. 2013;120(4):736–744.
18. Anctil JL, Anderson DR. Early foveal involvement and generalized depression of the visual field in glaucoma. *Arch Ophthalmol*. 1984;102(3):363–370.
19. Hood DC, Raza AS, de Moraes CGV, et al. Initial arcuate defects within the central 10 degrees in glaucoma. *Invest Ophthalmol Vis Sci*. 2011;52(2):940–946.
20. Hood DC, Raza AS, de Moraes CGV, Johnson CA, Liebmann JM, Ritch R. The nature of macular damage in glaucoma as revealed by averaging optical coherence tomography data. *Transl Vis Sci Technol*. 2012;1(1):3.
21. Chen S, McKendrick AM, Turpin A. Choosing two points to add to the 24-2 pattern to better describe macular visual field damage due to glaucoma. *Br J Ophthalmol*. 2015;99(9):1236–1239.
22. Hood DC, Slobodnick A, Raza AS, de Moraes CG, Teng CC, Ritch R. Early glaucoma involves both deep local, and shallow widespread, retinal nerve fiber damage of the macular region. *Invest Ophthalmol Vis Sci*. 2014;55(2):632–649.
23. Wang M, Hood DC, Cho JS, et al. Measurement of local retinal ganglion cell layer thickness in patients with glaucoma using frequency-domain optical coherence tomography. *Arch Ophthalmol*. 2009;127(7):875–881.
24. Wang DL, Raza AS, de Moraes CG, et al. Central glaucomatous damage of the macula can be overlooked by conventional OCT retinal nerve fiber layer thickness analyses. *Trans Vis Sci Tech*. 2015;4(6):4.
25. Cirafici P, Maiello G, Ancona C, Masala A, Traverso CE, Iester M. Point-wise correlations between 10-2 Humphrey visual field and OCT data in open angle glaucoma. *Eye*. 2021;35(3):868–876.
26. Shamsi F, Liu R, Owsley C, Kwon M. Identifying the retinal layers linked to human contrast sensitivity via deep learning. *Invest Ophthalmol Vis Sci*. 2022;63(2):27.
27. João CAR, Scanferla L, Jansonius NM. Binocular interactions in glaucoma patients with nonoverlapping visual field defects: Contrast summation, rivalry, and phase combination. *Invest Ophthalmol Vis Sci*. 2021;62(12):9.
28. Shamsi F, Liu R, Kwon M. Binocularly asymmetric crowding in glaucoma and a lack of binocular summation in crowding. *Invest Ophthalmol Vis Sci*. 2022;63(1):36.
29. Reche-Sainz JA, Gómez de Liaño R, Toledano-Fernández N, García-Sánchez J. Binocular vision in glaucoma. *Arch Soc Esp Oftalmol*. 2013;88(5):174–178.
30. Sheedy JE, Bailey IL, Buri M, Bass E. Binocular vs. monocular task performance. *Am J Optom Physiol Opt*. 1986;63(10):839–846.
31. Jones RK, Lee DN. Why two eyes are better than one: The two views of binocular vision. *J Exp Psychol Hum Percept Perform*. 1981;7(1):30–40.
32. Maiello G, Kwon M, Bex PJ. Three-dimensional binocular eye–hand coordination in normal vision and with simulated visual impairment. *Exp Brain Res*. 2018;236(3):691–709.
33. Bassi CJ, Galanis JC. Binocular visual impairment in glaucoma. *Ophthalmology*. 1991;98(9):1406–1411.
34. Essock EA, Fechtner RD, Zimmerman TJ, Krebs WK, Nussdorf JD. Binocular function in early glaucoma. *J Glaucoma*. 1996;5(6):395–405.
35. Gupta N, Krishnadev N, Hamstra SJ, Yücel YH. Depth perception deficits in glaucoma suspects. *Br J Ophthalmol*. 2006;90(8):979–981.
36. Parker AJ. Binocular depth perception and the cerebral cortex. *Nat Rev Neurosci*. 2007;8(5):379–391.
37. Maiello G, Chessa M, Bex PJ, Solari F. Near-optimal combination of disparity across a log-polar scaled visual field. *PLoS Comput Biol*. 2020;16(4):e1007699.
38. Prince SJD, Rogers BJ. Sensitivity to disparity corrugations in peripheral vision. *Vis Res*. 1998;38(17):2533–2537.
39. Lawlor M, Danesh-Meyer H, Levin LA, Davagnanam I, De Vita E, Plant GT. Glaucoma and the brain: Trans-synaptic degeneration, structural change, and implications for neuroprotection. *Surv Ophthalmol*. 2018;63(3):296–306.
40. Chan JW, Chan NC, Sadun AA. Glaucoma as neurodegeneration in the brain. *EB*. 2021;13:21–28.

Investigative Ophthalmology & Visual Science

41. You M, Rong R, Zeng Z, Xia X, Ji D. Transneuronal degeneration in the brain during glaucoma. *Front Aging Neurosci*. 2021;13:643685.
42. Nguyenkim JD, DeAngelis GC. Disparity-based coding of three-dimensional surface orientation by macaque middle temporal neurons. *J Neurosci*. 2003;23(18):7117–7128.
43. Jones PR. A tutorial on cue combination and signal detection theory: Using changes in sensitivity to evaluate how observers integrate sensory information. *J Math Psychol*. 2016;73:117–139.
44. Stewart EEM, Valsecchi M, Schütz AC. A review of interactions between peripheral and foveal vision. *J Vis*. 2020;20(12):2.
45. Blake A, Bülthoff HH, Sheinberg D. Shape from texture: Ideal observers and human psychophysics. *Vis Res*. 1993;33(12):1723–1737.
46. Ernst MO, Banks MS. Humans integrate visual and haptic information in a statistically optimal fashion. *Nature*. 2002;415(6870):429–433.
47. Landy MS, Maloney LT, Johnston EB, Young M. Measurement and modeling of depth cue combination: In defense of weak fusion. *Vis Res*. 1995;35(3):389–412.
48. Backus BT, Banks MS. Estimator reliability and distance scaling in stereoscopic slant perception. *Perception*. 1999;28(2):217–242.
49. van Beers RJ, Sittig AC, van der Gon JJD. Integration of proprioceptive and visual position-information: An experimentally supported model. *J Neurophysiol*. 1999;81(3):1355–1364.
50. Rohde M, van Dam LCJ, Ernst MO. Statistically optimal multisensory cue integration: A practical tutorial. *Multisens Res*. 2016;29(4–5):279–317.
51. Sample PA, Girkin CA, Zangwill LM, et al. The African Descent and Glaucoma Evaluation Study (ADAGES): Design and baseline data. *Arch Ophthalmol*. 2009;127(9):1136–1145.
52. Hodapp E, Parrish RK, Anderson DR. *Clinical Decisions in Glaucoma*. Maryland Heights: Mosby; 1993.
53. Brainard DH. The Psychophysics Toolbox. *Spat Vis*. 1997;10(4):433–436.
54. Pelli DG. The VideoToolbox software for visual psychophysics: Transforming numbers into movies. *Spat Vis*. 1997;10(4):437–442.
55. Reynaud A, Gao Y, Hess RF. A normative dataset on human global stereopsis using the quick Disparity Sensitivity Function (qDSF). *Vis Res*. 2015;113:97–103.
56. Georgeson MA, Yates TA, Schofield AJ. Discriminating depth in corrugated stereo surfaces: Facilitation by a pedestal is explained by removal of uncertainty. *Vis Res*. 2008;48(21):2321–2328.
57. Yang Q, Bucci MP, Kapoula Z. The latency of saccades, vergence, and combined eye movements in children and in adults. *Invest Ophthalmol Vis Sci*. 2002;43(9):2939–2949.
58. Baloh RW, Sills AW, Kumley WE, Honrubia V. Quantitative measurement of saccade amplitude, duration, and velocity. *Neurology*. 1975;25(11):1065–1065.
59. Volkmann FC. Vision during voluntary saccadic eye movements. *J Opt Soc Am*. 1962;52(5):571.
60. Dorr M, Bex PJ. Peri-saccadic natural vision. *J Neurosci*. 2013;33(3):1211–1217.
61. Wetherill GB, Levitt H. Sequential estimation of points on a psychometric function. *Br J Math Stat Psychol*. 1965;18(1):1–10.
62. Tyler CW. Spatial organization of binocular disparity sensitivity. *Vis Res*. 1975;15(5):583–590.
63. Bradshaw MF, Rogers BJ. Sensitivity to horizontal and vertical corrugations defined by binocular disparity. *Vis Res*. 1999;39(18):3049–3056.
64. Kim JM, Kyung H, Shim SH, Azarbod P, Caprioli J. Location of initial visual field defects in glaucoma and their modes of deterioration. *Invest Ophthalmol Vis Sci*. 2015;56(13):7956.
65. Crabb DP, Smith ND, Glen FC, Burton R, Garway-Heath DF. How does glaucoma look? Patient perception of visual field loss. *Ophthalmology*. 2013;120(6):1120–1126.
66. Hu CX, Zangalli C, Hsieh M, et al. What do patients with glaucoma see? Visual symptoms reported by patients with glaucoma. *Am J Med Sci*. 2014;348(5):403–409.
67. Xiong YZ, Liu R, Kwon M, Bittner AK, Owsley C, Legge GE. A unified rule for binocular contrast summation applies to normal vision and common eye diseases. *Invest Ophthalmol Vis Sci*. 2021;62(13):6.
68. Maiello G, Harrison WJ, Bex PJ. Monocular and binocular contributions to oculomotor plasticity. *Sci Rep*. 2016;6(1):31861.
69. Maiello G, Chessa M, Solari F, Bex PJ. The (in)effectiveness of simulated blur for depth perception in naturalistic images. *PLoS One*. 2015;10(10):e0140230.
70. Maiello G, Kerber KL, Thorn F, Bex PJ, Vera-Diaz FA. Vergence driven accommodation with simulated disparity in myopia and emmetropia. *Exp Eye Res*. 2018;166:96–105.
71. Maiello G, Schepko M, Klein LK, Paulun VC, Fleming RW. Humans can visually judge grasp quality and refine their judgments through visual and haptic feedback. *Front Neurosci*. 2021;14:591898.
72. Caoli A, Sabatini SP, Gibaldi A, Maiello G, Kosovicheva A, Bex P. A dichoptic feedback-based oculomotor training method to manipulate interocular alignment. *Sci Rep*. 2020;10(1):15634.
73. Chessa M, Maiello G, Bex PJ, Solari F. A space-variant model for motion interpretation across the visual field. *J Vis*. 2016;16(2):12.
74. Rosa R, Corazza P, Musolino M, et al. Choroidal changes in intermediate age-related macular degeneration patients with drusen or pseudodrusen. *Eur J Ophthalmol*. 2021;31(2):505–513.

Investigative Ophthalmology & Visual Science